J|A|C|S
COMMUNICATIONS

Published on Web 12/21/2006

Dynamic Assembly by Electrokinetic Microfluidics

Shengnian Wang,[†] Xin Hu,[‡] and L. James Lee*,[†]

Departments of Chemical and Biomolecular Engineering and Mechanical Engineering, The Ohio State University, Columbus, Ohio 43210

Received September 18, 2006; E-mail: lee.31@osu.edu

Self-assembly is well-known for creating nanoscale or molecular scale patterns with simple forms (thin films, particles, or fibers).[1−3] In conjunction with "Templates Synthesis", self-assembly can provide many useful nanostructures (e.g., nanowires, nanorods, and nanotubules) by constrained assembly on a template.[4−7] However, this approach is slow and it is difficult to produce multifunctional structures in deep channels. External forces such as pressure, magnetism, and capillary forces have been successfully used to assist the assembly process on a two-dimensional flat surface.[8−10]

Electrochemical processes like electroforming and anodization, on the other hand, can continuously bring fresh reactants (i.e., ions) toward the reaction interface (one electrode) by electric force.[11,12] They are widely used in the production of metal molds/stampers for microfabrication. By combining self-assembly and electrochemical forming concepts, we have recently demonstrated that silica assembly on the surface of conically shaped nanochannels (nanonozzle array) can be achieved by electrokinetic flows (EKF).[13,14] Unlike electroforming where the electrolytes migrate from one electrode to the other and deposit, an electrostatically charged nanofluidic template is placed between the two electrodes in our dynamic assembly process such that electrolytes can be intercepted on the template surface. Silica was successfully grown on a nanochannel surface, yielding further size reduction and mechanical property reinforcement.

In this study, we further investigate this EKF-induced dynamic assembly process in a two-dimensional converging microchannel, which is 300 μm long, 40 μm deep, and 20 μm wide at the small end and 130 μm at the large end. Polymeric (e.g., polyethylene terephthalate (PET) and polymethyl methacrylate (PMMA)) channels were fabricated by photolithography followed by hot embossing. Poly(allyamine hydrochloride, PAH, Mv = 720000) was anchored onto the polymer channel surface by polyelectrolyte multilayer (PEM) deposition to form a positively charged surface.[15] Negatively charged polystyrene nanoparticles with fluorescence (40 nm, Polysciences) were used for assembly with the $d_{particle}/D_{small\ end}$ ratio equal to 0.0025, similar to the nanonozzle arrays used in our silica assembly study. The dynamic assembly was carried out by applying a 60 V/cm electric bias across the converging channel (from the large end to the small end). The process was recorded using inverted fluorescence microscopy (TE2000S, Nikon, Japan) with a 12-bit high-resolution camera (CoolSNAP HQ, Roper Scientific), and the flow pattern was visualized in a way widely used by other researchers.[16] The fluorescence intensity along the channel wall was also measured to determine the extent of nanoparticle deposition on the solid surface.

A pair of lip vortices was observed outside the small end, while a pair of double vortices was formed near the wall inside the tapered channel during the dynamic assembly process (Figure 1). Strong hydrodynamic interactions and electroosmotic flow (EO) at the small end of the channel are believed to be the main reasons for the formation of lip vortices and their direction of circulation. The formation of the wall vortex and its direction of circulation inside the converging channel comes from the interactions of electrophoresis (EP) of charged species, electroosmotic flow (EO) from charged channel surface, and the induced pressure-driven backflow. A detailed mechanism of the vortex formation is described elsewhere.[17] The initial lip and wall vortex directions of circulation are shown in Figure 2I when the channel surface is positively charged. The lip vortices slowed down the particle movement, allowing deposition near the lip area. At the same time, the main flow in the center of the channel continuously brought fresh reactants to the vortices and prevented the channel from blocking by particles. As a result, the surface ζ-potential at the small end became less positive and gradually changed to negative when nanoparticles were continually deposited. A ζ-potential gradient appeared along the channel surface leading to the formation of new vortices near the small end (Figure 2II). A stagnation point (or a stagnation plane if considering the depth direction in the 3D flow) was formed at the location where the new vortex met the existing vortex. Some nanoparticles in the circulation flow fell into this region, leading to the primary assembly between

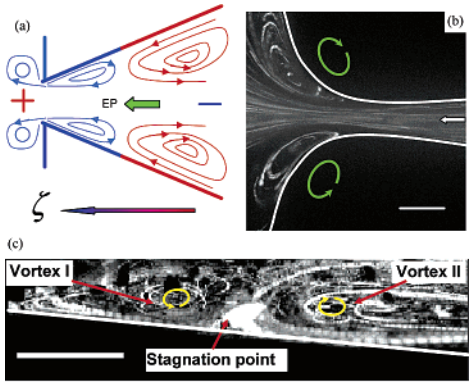

Figure 1. (a) Schematic and the streak images of (b) lip vortex near the small end, and (c) a double vortex inside the converging channel. Channel edges are outlined for clarity and the scale bars in panels b and c present 20 μm and 200 μm, respectively.

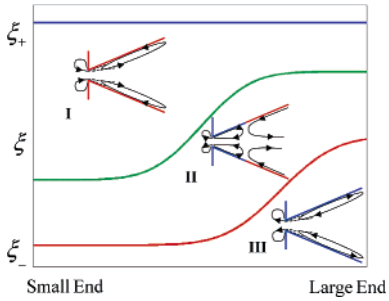

Figure 2. The evolution of surface ζ-potential distribution and associated vortex flow patterns in dynamic assembly: (I) initially uniform positively charged surface, (II) negatively and positively charged zones formed with double vortex, and (III) negatively charged zone covering the entire channel surface.

[†] Department of Chemical and Biomolecular Engineering.
[‡] Department of Mechanical Engineering.

10.1021/ja0666295 CCC: $37.00

the PAH layer and nanoparticles because stagnation provided little motion and a long residence time for nanoparticles. As more particles were deposited, the ζ-potential profile on the channel surface kept changing. This double vortex gradually moved toward the large end, resulting in the migration of the stagnation interface, or the frontline of the primary dynamic assembly. The compounded trajectory profile of the double vortex in Figure 1c shows such migration. Although multiple vortex circulation has been reported by using patterned surface charge or nonplanar surface topography,[18,19] our results showed, for the first time, the moving double vortex and its application to dynamic assembly. The assembly continued after the stagnation region moved away because of the presence of the wall vortex. Compared to the primary assembly, the assembly rate resulting from the wall vortex alone was much lower because nanoparticles were brought near the surface by the recirculation flow, not by the stagnation. Also, the channel surface behind the assembly front became less effective for further electrostatic deposition as the surface charge changed from positive to negative. Eventually, the entire channel surface charge turned to negative and the double vortex disappeared. The lip and wall vortices circulated in opposite directions (Figure 2III), compared to the initial condition. Using fluorescence labeled nanoparticles, this dynamic assembly process was clearly observed under microscopy (see the movie in Supporting Information). The measured fluorescence intensity at four different locations along the converging channel surface is given in Figure 3a, where the solid content of nanoparticles in the suspension was about 0.00118 wt %, and the suspension was continuously supplied. The assembly started from the small end and extended gradually toward the large end. Near the small end, there was a rapid growth stage (primary assembly) followed by a much slower one (secondary assembly). For the surface assembly starting early, its final assembly level was caught up sequentially by the surface where the assembly was delayed for various periods. Eventually the assembly along the whole channel surface would reach a uniform and saturated level. The two-stage assembly was pronounced near the small end and became less clear when approaching the large end.

Even though uniform assembly is useful, gradient and multimaterial assembly can also be attractive.[20] This can be achieved by using either concentrated suspensions, a gradient PAH surface, pulsatile feeding, periodic electric pulses, or a combination of these. Anchoring polyelectrolyte molecules on the channel surface by dynamic assembly can generate a gradient surface ζ-potential distribution for further assembly. The pulsatile feeding and periodic electric pulses can limit the assembly only at its early stage (i.e., the primary assembly). Figure 3b shows the results of feeding the converging microchannel with either single or multiple doses of 1 μL nanoparticle suspension having a solid content of 0.0118 wt %. For single dose feeding, the assembly achieved a similar level of deposition as in the continuous feeding case near the small end, while much less deposition was achieved in other regions because of the quick exhaust of nanoparticles. The difference in assembly level along the channel surface was amplified when multiple dosages were fed. In this simple way for gradient assembly, the dosage interval and the suspension concentration in each dose were found to be the two key factors controlling this particular gradient assembly process. A shorter dosage interval approaches continuous feeding, with a more uniform assembly. Since the surface properties can be tailored, this gradient assembly method can be used in combinatorial techniques for drug discovery and material sciences.[21] It can also be used to deposit various functional materials at different locations in micro- and nanoscale constructs.

In summary, dynamic assembly assisted by electrokinetic flows was carried out with PS nanoparticles deposited along a two-dimensional converging channel surface. A two-stage assembly was observed owing to the migrating double vortex in the channel. The assembly started from the small end of the converging channel and extended gradually toward the large end. Continuous feeding of diluted suspensions provides a uniform deposition on the channel surface, while the feeding of multiple dosages can result in gradient or multimaterial assembly.

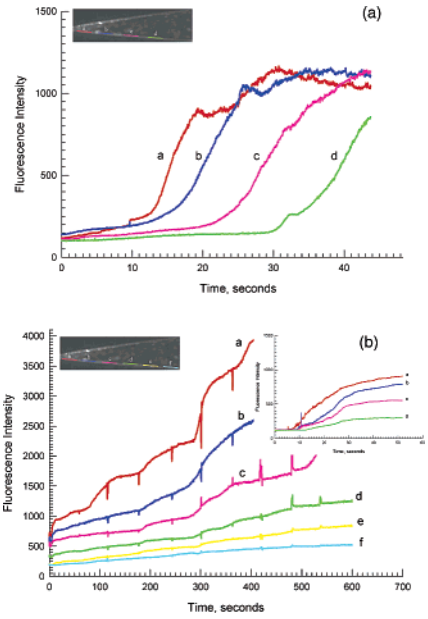

Figure 3. Growth curves of dynamic assembly (a) continuous feeding and (b) multiple dosages feeding with the insert figure for feeding with single dose. Letters a−f label different locations on the surface of the converging channel, starting with "a" near the small end. The fluorescence intensity correlates with the amount of nanoparticle deposition.

Acknowledgment. The authors thank the NSF Center for Affordable Nanoengineering of Polymeric Biomedical Devices for financial support (Grant No. EEC-0425626).

Supporting Information Available: Movies (avi) and figures of this dynamic assembly process. This material is available free of charge via the Internet at http://pubs.acs.org.

References

(1) Whitesides, G. M.; Grzybowski, B. *Science* **1997**, *295*, 2418.
(2) Decher, G. *Science* **1997**, *277*, 1232.
(3) Forster, S.; Plantenberg, T. *Angew. Chem., Int. Ed.* **2002**, *41*, 688.
(4) Thurn-Albrecht, T.; Schotter, J.; Kastle, G. A.; Emley, N.; Shibauchi, T.; Krusin-Elbaum, L.; Guarini, K.; Black, C. T.; Tuominen, M. T.; Russell, T. P. *Science* **2000**, *290*, 2126.
(5) Kyotani, T.; Tsai, L. F.; Tomita, A. *Chem. Mater.* **1996**, *8*, 2109.
(6) Fan, R.; Wu, Y.; Li, D.; Yue, M.; Majumdar, A.; Yang, P. *J. Am. Chem. Soc.* **2003**, *125*, 5254.
(7) Jirage, K. B.; Hulteen, J. C.; Martin, C. R. *Science* **1997**, *278*, 655.
(8) Ganguly, R.; Zellmer, B.; Puri, I. K. *Phys. Fluids.* **2005**, *17*, 097104.
(9) Cademartiri, L.; Sutti, A.; Calestani, G. *Langmuir* **2003**, *19*, 7944.
(10) Gates, B.; Qin, D.; Xia, Y. *Adv. Mater.* **1999**, *11*, 466.
(11) Madou, M. J. *Fundamental of Microfabrication*; CRC Press: Boca Raton, FL, 1997.
(12) Sadasivan, V.; Richter, C. P.; Menon, C.; William, P. F. *AIChE J.* **2005**, *51*, 649.
(13) Wang, S.; Zeng, C.; Lai, S.; Juang, Y.-J.; Yang, Y.; Lee, L. J. *Adv. Mater*, **2005**, *17*, 1182.
(14) Zeng, C.; Wang, S.; Lee, L. J. *Mater. Lett.* **2005**, *59*, 3095.
(15) Chen, W.; McCarthy, T. J. *Macromolecules* **1997**, *30*, 78.
(16) Hu, H; Larson, R. G. *J. Phys. Chem. B* **2006**, *110*, 7090.
(17) Wang, S.; Hu, X.; Lee, L. J. Unpublished work.
(18) Stroock, A. D.; Weck, M.; Chiu, D. T.; Huck, W. T. S.; Kenis, P. J. A.; Ismagilov, R. F.; Whitesides, G. M. *Phys. Rev. Lett.* **2000**, *84*, 3314.
(19) Lettieri, G.-L.; Dodge, A.; Boer, G.; de Rooij, N. F.; Verpoorte, E. *Lab Chip* **2003**, *3*, 34.
(20) Caelen, I.; Bernard, A.; Juncker, D.; Michel, B.; Heinzelmann, H.; Delamarche, E. *Langmuir* **2000**, *16*, 9125.
(21) Meredith, J. C.; Karim, A.; Amis, E. J. *MRS Bull.* **2002**, *27*, 330.

JA0666295